

## Focusing a helium atom beam using a quantum-reflection mirror

This article has been downloaded from IOPscience. Please scroll down to see the full text article.

2009 New J. Phys. 11 113030

(<http://iopscience.iop.org/1367-2630/11/11/113030>)

View [the table of contents for this issue](#), or go to the [journal homepage](#) for more

Download details:

IP Address: 141.14.132.170

The article was downloaded on 12/03/2012 at 14:08

Please note that [terms and conditions apply](#).

## Focusing a helium atom beam using a quantum-reflection mirror

H Christian Schewe, Bum Suk Zhao<sup>1</sup>, Gerard Meijer and Wieland Schöllkopf

Fritz-Haber-Institut der Max-Planck-Gesellschaft, Faradayweg 4-6,  
14195 Berlin, Germany

E-mail: [zhao@fhi-berlin.mpg.de](mailto:zhao@fhi-berlin.mpg.de)

*New Journal of Physics* **11** (2009) 113030 (10pp)

Received 23 July 2009

Published 17 November 2009

Online at <http://www.njp.org/>

doi:10.1088/1367-2630/11/11/113030

**Abstract.** We demonstrate one-dimensional (1D) focusing of a thermal helium atom beam by quantum reflection from a cylindrical concave quartz mirror at near-grazing incidence. The smallest width of the focus achieved is  $1.8\ \mu\text{m}$ , essentially limited by spherical aberration. The various effects that contribute to the finite focal width have been investigated. We propose to apply near-grazing reflection from two concave elliptical mirrors in a Kirkpatrick–Baez arrangement for two-dimensional (2D) focusing of a helium atom beam, paving the way for a helium atom microprobe.

### Contents

<b>1. Introduction</b>	<b>2</b>
<b>2. Experimental setup</b>	<b>3</b>
<b>3. Results and discussion</b>	<b>4</b>
3.1. Reflection probability of the mirror . . . . .	4
3.2. Focused beam profiles . . . . .	5
3.3. Factors determining the focal width . . . . .	6
<b>4. Conclusions and outlook</b>	<b>8</b>
<b>Acknowledgments</b>	<b>9</b>
<b>References</b>	<b>9</b>

<sup>1</sup> Author to whom any correspondence should be addressed.

## 1. Introduction

Focusing microscopy, such as optical microscopy and scanning electron microscopy, is indispensable in modern science. In the last decade, helium atoms have attracted attention as a possible means to perform matter-wave microscopy with [1]–[6]. There have been two approaches to focus neutral helium atoms, i.e. in transmission using Fresnel zone plates, and in reflection using a curved surface. Metastable helium atoms were focused by a commercial Fresnel zone plate in 1991 [1]. This method has been optimized for ground-state helium atoms by using custom-made zone plates and micro-skimmers [7]. With a 1- $\mu\text{m}$ -diameter skimmer a focused spot diameter of 2  $\mu\text{m}$  was achieved [3]. Recently, this achievement was extended to two-dimensional (2D) imaging with helium atoms [6]. Since focusing with Fresnel zone plates is based on diffraction, chromatic aberration is an inherent problem and sets a limit to the diameter of the focused spot. Moreover, unfocused zeroth-order and defocused first-order diffraction induce high levels of background signals, comparable in magnitude to those of the focused first-order signal.

Various reflection mechanisms have been exploited to focus neutral atoms by reflection from curved surfaces. One of them is based on quantum reflection of hydrogen atoms from a liquid helium surface [8, 9]. Hydrogen atom beams emerging from a 500  $\mu\text{m}$  pinhole were focused back into it by a concave mirror coated with liquid helium [10]. Furthermore, helium atom scattering from microscopically smooth crystal surfaces has been studied for decades [14], and has been used to focus helium atom beams by coherent reflection from a concave silicon membrane into a 210  $\mu\text{m}$  focal spot [2]. This was the first reflection mechanism considered for the realization of a scanning helium microscope [4]. More recently, Fresnel diffraction from nanoscale ridges structured on a surface was observed to result in large reflection probabilities for metastable helium and neon atoms [15], and this mechanism has also been discussed in view of its applicability in an atomic nanoscope [5]. Additionally, focusing of cold atoms released from a magneto-optical trap was demonstrated by reflection from a concave surface based on optical [11] or magnetic [12] dipole forces. In addition, gravity was exploited for one-dimensional (1D) focusing of cold atoms quantum reflected from a flat surface [13].

In the experiments described here, we exploit quantum reflection from a concave, microscopically rough quartz surface at near-grazing incidence to focus thermal helium atom beams. Quantum reflection from the attractive branch of the Van der Waals atom–surface interaction has been observed experimentally [16] and investigated theoretically [17]. More recently, quantum reflection of helium atom beams from solid surfaces has been reported [18]–[20]. Quantum reflection takes place tens of nanometers away from the surface and is hardly affected by the surface roughness. Therefore, the complication of preparing and maintaining microscopically flat surfaces is avoided [20].

An important requirement for a mirror for helium atom beam focusing is to have a regularly curved macroscopic shape to minimize aberrations. This is challenging to achieve for bent silicon crystal membranes [4]. We propose here to take advantage of Kirkpatrick–Baez (KB) optics—developed originally for x-ray focusing [21]—for 2D focusing of helium atom beams. Kirkpatrick and Baez proposed focusing of x-rays at grazing incidence with two crossed cylindrical concave mirrors [21]. Total external reflection at near-grazing incidence provides large reflectivity of x-rays. To avoid the problem of astigmatism from a single spherical mirror at grazing incidence, two cylindrical mirrors are used. KB optics for focusing x-ray beams has found widespread use at synchrotron radiation facilities around the world. Recently, the

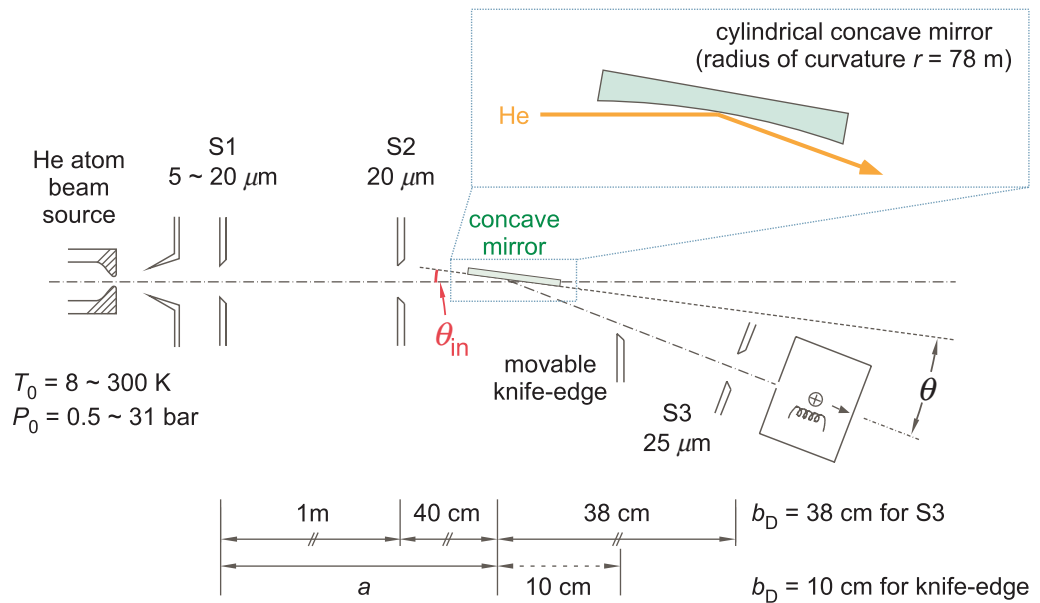


**Figure 1.** Scheme of the experimental setup. Two different image planes are relevant for two different detection schemes. In the first scheme, angular profiles are recorded by scanning S3 located 38 cm downstream from the mirror center around an angle  $\theta$ . In the second scheme, a silicon knife-edge is translated through the beam profile at 10 cm downstream from the mirror center with the slit S3 removed and with the detection angle  $\theta$  fixed at the specular angle.

resolution of this technique has been improved to below 100 nm by using elliptical mirrors instead of cylindrical ones [22, 23]. Near-grazing incidence is also essential to increase the reflectivity in quantum reflection of thermal helium atom beams [19]. Therefore, many techniques and theories developed for KB optics can be applied to helium atom beam focusing. Furthermore, the reflection is free from chromatic aberration and the background signal only results from unfocused diffusive scattering, which is small relative to the intensity of the specularly reflected beam.

Here, we demonstrate 1D focusing of a thermal helium atom beam by a single cylindrical concave mirror. We study the various factors affecting the obtainable focal width by controlling the experimental conditions, such as the effective size of the helium beam source, the de Broglie wavelength of the helium atoms, and the distance between the mirror and the image plane.

## 2. Experimental setup

The helium beam apparatus is the same as the one used in a previous experiment [19]. The continuous atom beam is formed in a supersonic expansion of helium gas at a stagnation temperature  $T_0$  and pressure  $P_0$  through a 5- $\mu\text{m}$ -diameter orifice into high vacuum. After passing through a skimmer of 500  $\mu\text{m}$  diameter, the beam is collimated by two slits (S1 and S2) separated by 100 cm as indicated in figure 1. The first slit S1 can be assigned a fixed nominal width  $w_{S1}$  of  $5 \pm 1$ ,  $10 \pm 1$ , or  $20 \pm 2 \mu\text{m}$ , while the width of S2 is fixed to  $w_{S2} = 20 \pm 2 \mu\text{m}$ . The second slit is located 40 cm upstream from the (vertical) pivot axis of

the precisely rotatable mirror mount. The detector consists of an electron-impact ionization mass spectrometer behind a 25- $\mu\text{m}$ -wide detector-entrance slit (S3), located 38 cm downstream from the pivot axis. The cylindrical concave mirror is positioned at the crossing point of the atom-beam axis and the pivot axis so that the latter is parallel to the flat direction of the mirror and passes through its center. The grazing incidence angle  $\theta_{\text{in}}$  and the detection angle  $\theta$  are measured with respect to the tangential plane at the mirror center. Angular profiles of incident and reflected atom beams are measured by rotating the detector and measuring the He signal as a function of  $\theta$ .

In a second measuring mode, a piezo-driven silicon knife-edge that can be moved into the beam path 10 cm downstream from the mirror center is used. In this mode the detector is fixed at the specular angle ( $\theta = \theta_{\text{in}}$ ) and the entrance slit S3 is removed so that all atoms passing by the knife edge pass into the detector. Scanning the knife edge through the helium beam allows us to determine the beam profile to within an accuracy of tens of nanometers.

As the mean kinetic energy of the atoms depends on  $T_0$ , the mean de Broglie wavelength  $\lambda_{\text{dB}}$  can be increased by cooling the source. In this work stagnation temperatures of  $T_0 = 300, 120, 50.4$  and  $8.7$  K (stabilized to  $\pm 0.01$  K) were used corresponding to de Broglie wavelengths of  $\lambda_{\text{dB}} = 0.56, 0.89, 1.38$  and  $3.45$  Å, respectively. The relative wavelength spread of about 1% or less [24] is negligible with respect to the effects studied in this work.

In analogy with classical optics we introduce the source-to-mirror distance  $a$  and the mirror-to-image-plane distance  $b$ . As indicated in figure 1, we approximate  $a$  by the distance between S1 and the mirror center,  $a = 140$  cm; the effective source size of the helium atom beam is limited by the first slit and we approximate it by  $w_{\text{S1}}$  [25]. We define  $b_{\text{D}}$  as the distance from the mirror center to the detection plane, i.e.  $b_{\text{D}} = 10$  or  $38$  cm when the knife-edge or the slit S3 is used, respectively.

The commercially available cylindrical mirror is made out of 10 mm thick quartz and has dimensions of  $50 \times 50$  mm<sup>2</sup>. Its concave surface is characterized by a nominal radius of curvature of  $R = 78$  m  $\pm 1\%$ . The mirror is mounted into vacuum without *ex situ* or *in situ* preparation. The focal length  $f$  of a concave mirror is a function of incidence angle via  $f(\theta_{\text{in}}) = R \sin \theta_{\text{in}}/2$  [21]. Therefore, the focal length of our mirror at incidence angles below 10 mrad is only a few tens of centimeters, and the focal point is located inside of the experimental setup, fulfilling the thin lens equation,  $1/a + 1/b = 1/f(\theta_{\text{in}})$ . With  $a$  being fixed in our setup, we vary  $\theta_{\text{in}}$  to match  $b$  and  $b_{\text{D}}$  to image the helium atom beam source in either one of the two detection planes.

### 3. Results and discussion

#### 3.1. Reflection probability of the mirror

The coherent reflection probability of the mirror depends on the helium beam velocity and hence on  $\lambda_{\text{dB}}$ , and is a steeply decreasing function of incidence angle  $\theta_{\text{in}}$  [19, 20]. There is evidence from further experiments for a transition of the underlying reflection mechanism from *quantum reflection* at small  $\theta_{\text{in}}$  to *classical reflection* at larger  $\theta_{\text{in}}$ . This will be detailed in a separate publication [20]. For the experimental conditions of the present work both mechanisms contribute to the reflectivity. Either mechanism is effective only at near-grazing incidence; quantum reflection decays quickly with increasing wave-vector normal component, and classical reflection is strongly suppressed due to surface roughness unless the latter is

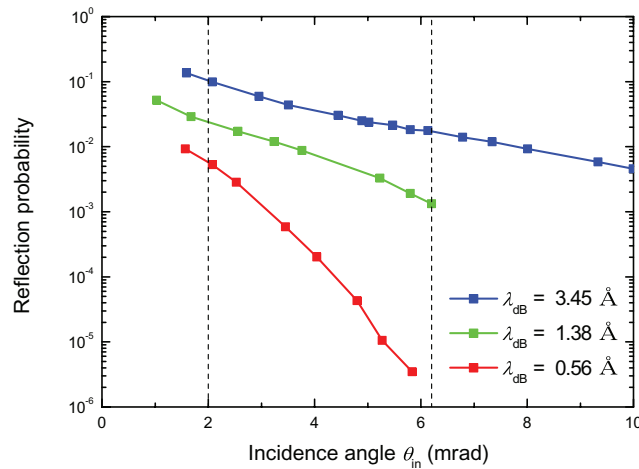


**Figure 2.** Observed coherent reflection probability of the helium atom beam versus incidence angle for three beam energies. The lines connecting data points are only guides to the eye. The dashed vertical lines indicate the incidence angles  $\theta_{in} = 2.0$  and  $6.2$  mrad that have been used for focusing in either one of the detection planes.

effectively averaged out at near-grazing incidence. Hence, grazing incidence is prerequisite for effective coherent reflection from a rough surface.

As can be seen in figure 2, the observed reflection probability varies over five orders of magnitude. The dashed lines in the figure indicate the incidence angles used for focusing in either one of the detection planes. For  $\theta_{in} = 2.0$  mrad, reflection probabilities of 10, 2.2 and 0.6% are found for  $\lambda_{dB} = 3.45$ , 1.38 and  $0.56 \text{ \AA}$ , respectively, while for  $\theta_{in} = 6.2$  mrad 1.7 and 0.13% of the helium atom beam is reflected for  $\lambda_{dB} = 3.45$  and  $1.38 \text{ \AA}$ , respectively.

### 3.2. Focused beam profiles

Figure 3 shows focused helium atom beam profiles observed by (a) rotating S3 and by (b) scanning the knife-edge. In either measurement the incidence angle  $\theta_{in}$  was adjusted so that the focal plane of the mirror coincided with the detection plane, i.e. the plane of S3 and the knife-edge. In the first measurement the stagnation temperature was set to  $T_0 = 8.7 \text{ K}$ , corresponding to  $\lambda_{dB} = 3.45 \text{ \AA}$ , and the width of S1 was  $w_{S1} = 5 \mu\text{m}$ . Since the focused beam width is significantly smaller than the width of S3, a plateau appears at the center of the measured angular profile and the information concerning the actual focused beam profile is implied in the slopes. The deconvoluted focused beam profile can be obtained from the derivative of the data depicted in figure 3(c). The derivative curve is then fitted by two Gaussian functions providing two widths ( $W_+$  and  $W_-$ ) and two peak positions ( $\theta_+$  and  $\theta_-$ ) for the positive and negative peaks. The averaged full-width at half-maximum (FWHM)  $W = (W_+ + W_-)/2$  is  $10.7 \mu\text{rad}$ . With a known distance from S3 to the pivot axis of 38 cm this translates into a width of the focused beam of  $4.1 \pm 0.2 \mu\text{m}$ . The detection angle of the focused beam is determined from the average of both Gaussians to be  $\theta = (\theta_+ + \theta_-)/2 = 6.34 \text{ mrad}$ . The angular separation between the two peak positions is  $73 \mu\text{rad}$ , corresponding to  $27.6 \mu\text{m}$  in the plane of S3. This is in agreement with the nominal width of S3 ( $25 \pm 2 \mu\text{m}$ ) within its uncertainty limit.

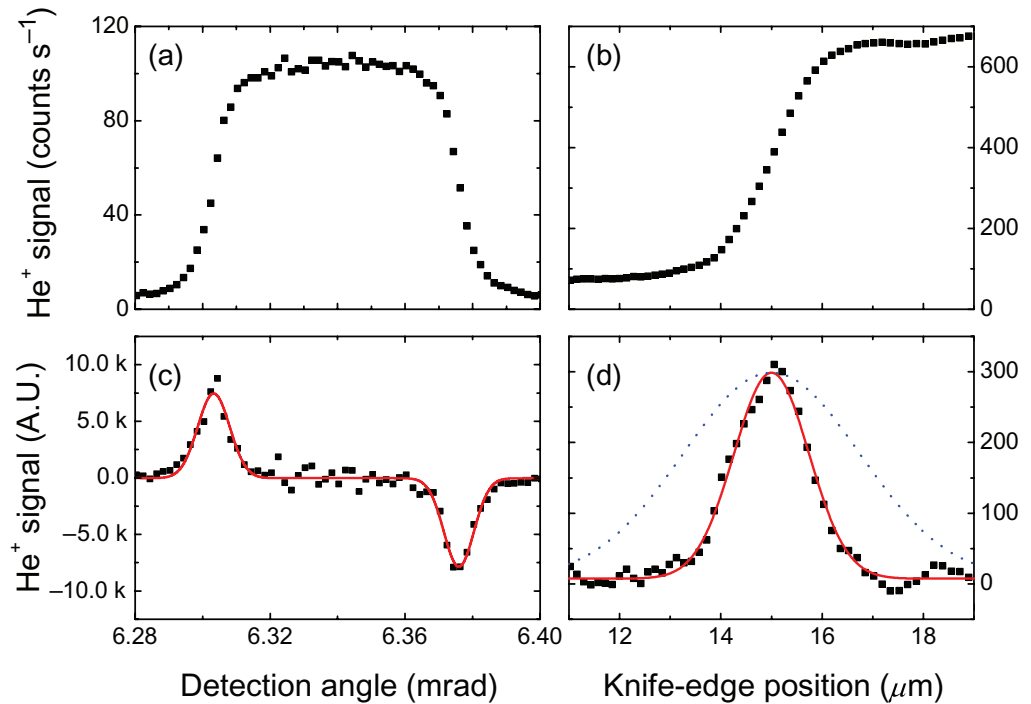


**Figure 3.** Measured profiles of helium atom beams focused by the concave mirror at (a) 38 cm and (b) 10 cm downstream from the mirror. Derivatives of these profiles are presented in (c) and (d), respectively. The solid lines are Gaussian fits to the derivatives. For comparison, a normalized Gaussian curve, using the fitting parameters obtained from (c), is depicted in (d) as the dotted curve.

In the second measurement, with the knife-edge, the detection angle  $\theta$  was fixed at 1.9 mrad, with S3 removed. In this measurement the width of S1 was again  $w_{S1} = 5 \mu\text{m}$ , whereas  $\lambda_{dB}$  was set to 1.38 Å. The profile of the focused helium beam was again obtained by differentiating the measured curve, as shown in figure 3(d). The derivative is fitted by a Gaussian function, with a FWHM of  $W = 1.8 \pm 0.1 \mu\text{m}$ . For comparison with the S3 measurement, the Gaussian curve of figure (c) is plotted in (d) as well (dotted curve) with peak height and background level adjusted. The width of the focus 10 cm downstream from the mirror is about half of the width at 38 cm. This decrease results mainly from the geometrical demagnification of the atom beam source, but is less than expected from the thin lens formula by approximately a factor of two. The factors limiting the minimum obtainable focus are investigated in the following.

### 3.3. Factors determining the focal width

With the detection planes fixed at either  $b_D = 38 \text{ cm}$  or  $10 \text{ cm}$ , the spatial profiles of the atom beam have been measured at various incidence angles, as shown in figure 4. When the incidence angle  $\theta_{in}$  is adjusted from 1 to 10 mrad,  $b$  is increased from 4 to 54 cm. When  $b$  is close to  $b_D$ , the atom beam is properly focused and has the smallest FWHM ( $W_f$ ) in the detection plane; when  $b < b_D$  and  $b > b_D$ , the beam is over-focused and under-focused in the detection plane, respectively. In the measurement with  $b_D = 38 \text{ cm}$  in figures 4(a) and (c), the minimum  $W_f$

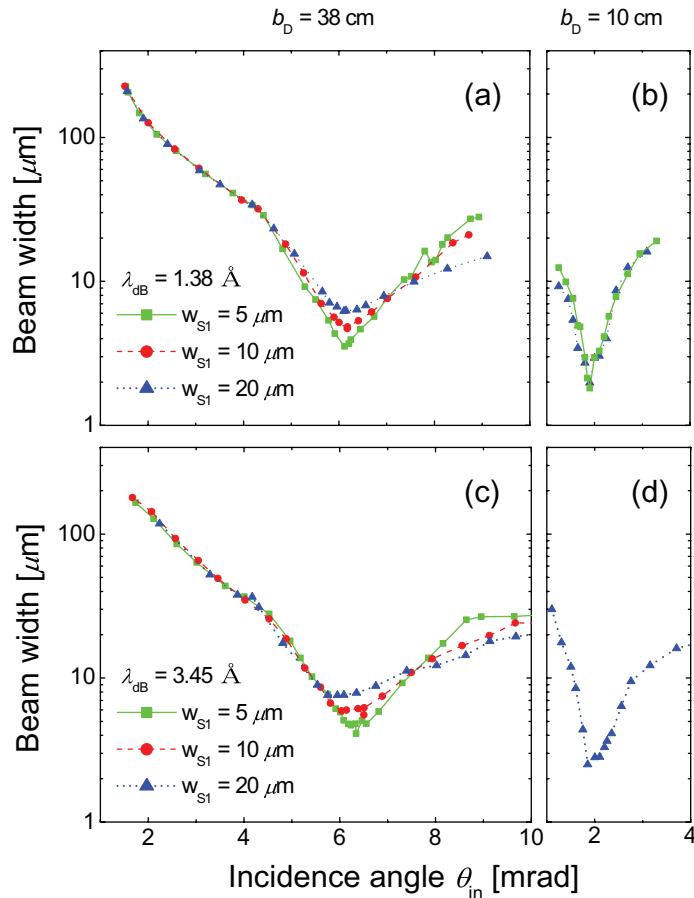


**Figure 4.** Observed widths of the helium atom beam versus incidence angle for three different effective source sizes  $w_{S1}$ , at de Broglie wavelengths of  $\lambda_{dB} = 1.38 \text{ \AA}$  ((a) and (b)) and  $3.45 \text{ \AA}$  ((c) and (d)). The distance to the detection plane,  $b_D$ , is fixed to 38 cm ((a) and (c)) and 10 cm ((b) and (d)).

is found for an incidence angle  $\theta_{in}$  of about 6.2 mrad. The dependence of the focused beam size  $W_f$  on the effective source size, which is determined by the first collimation slit, has been studied by changing the width of S1 ( $w_{S1}$ ) from 5 to 10 and 20  $\mu\text{m}$ . The minimum width  $W_f$  increases as the width of S1 gets larger;  $W_f$  increases from 4.1 to 7.6  $\mu\text{m}$  and from 3.5 to 6.2  $\mu\text{m}$  for  $\lambda_{dB} = 3.45 \text{ \AA}$  and  $1.38 \text{ \AA}$ , respectively, as  $w_{S1}$  increases from 5 to 20  $\mu\text{m}$ . This is expected because the focused beam size is proportional to the source (or object) size, as given by the simple geometric optical relation,  $W_{GO} = w_{S1}(b_D/a)$ .

In the measurement at  $b_D = 10 \text{ cm}$  the smallest widths are found near  $\theta_{in} = 2.0 \text{ mrad}$ . For  $\lambda_{dB} = 1.38 \text{ \AA}$  the minimum values are  $W_f = 1.8$  and  $2.0 \mu\text{m}$  when  $w_{S1} = 5$  and  $20 \mu\text{m}$ , respectively, which are the same within experimental error. Spherical aberration is the main reason for this; at small incidence angles, the helium atom beam covers a large area on the spherical mirror, resulting in large spherical aberration. The focal widths limited by the spherical aberration,  $W_{SA}$ , are calculated to be 1.81 and  $0.17 \mu\text{m}$  for  $b_D = 10$  and  $38 \text{ cm}$ , respectively [21].

The measured minimum widths of the focused beam,  $W_f$ , are summarized in table 1. Comparing the listed values on the same row, i.e. for a given  $w_{S1}$ , we see that the focal spot size is

**Table 1.** Minimum spot widths  $W_f$  in  $\mu\text{m}$  observed at the two detection planes. The error of the measured widths is less than 5%. Numbers in parentheses are calculated widths given by  $\sqrt{W_{\text{GO}}^2 + W_{\text{Diff}}^2 + W_{\text{SA}}^2}$ , with the individual contributions indicated by colors.

$w_{\text{S1}}$ ( $\mu\text{m}$ )	$\lambda_{\text{dB}} = 3.45 \text{ \AA}$	$b_{\text{D}} = 38 \text{ cm}$	
		$1.38 \text{ \AA}$	$0.89 \text{ \AA}$
5	4.1 (6.7 <sub>1.4,6.6,0.17</sub> )	3.5 (3.0 <sub>1.4,2.6,0.17</sub> )	
10	5.5 (7.1 <sub>2.7,6.6,0.17</sub> )	4.7 (3.8 <sub>2.7,2.6,0.17</sub> )	
20	7.6 (8.5 <sub>5.4,6.6,0.17</sub> )	6.2 (6.0 <sub>5.4,2.6,0.17</sub> )	5.9 (5.7 <sub>5.4,1.7,0.17</sub> )
$w_{\text{S1}}$ ( $\mu\text{m}$ )	$\lambda_{\text{dB}} = 3.45 \text{ \AA}$	$b_{\text{D}} = 10 \text{ cm}$	
		$1.38 \text{ \AA}$	$0.56 \text{ \AA}$
5	2.5 (2.5 <sub>0.36,1.7,1.8</sub> )	1.8 (2.0 <sub>0.36,0.69,1.8</sub> )	1.8 (1.9 <sub>0.36,0.28,1.8</sub> )
10			
20		2.0 (2.4 <sub>1.4,0.69,1.8</sub> )	

larger for larger values of  $\lambda_{\text{dB}}$ . This is due to the diffraction that occurs at slit S2. The diffraction limited focal width  $W_{\text{Diff}}$  is given by  $W_{\text{Diff}} = b_{\text{D}}\lambda_{\text{dB}}/w_{\text{S2}}$ . Diffraction is negligible compared to spherical aberration at  $b_{\text{D}} = 10 \text{ cm}$ , as can be seen from the data. The values in parentheses are the spot sizes calculated by convoluting the diffraction-limited spot size with the one obtained from geometrical optics,  $W_{\text{GO}}$ , and the one resulting from broadening due to spherical aberration,  $W_{\text{SA}}$ . The experimental data and the theoretical calculations are in good agreement.

With given positions of the source, the mirror, and the image plane, the important factors limiting the spot width are, therefore, the effective source size, diffraction at slit S2, and spherical aberration. Shifting the image plane closer to the mirror decreases the magnification factor  $b_{\text{D}}/a$  and also diminishes the effect of diffraction. However, with the cylindrical mirror a small value of  $b_{\text{D}}$  requires a small incidence angle and results in substantial spherical aberration, since a large area of the mirror is illuminated by the atom beam at small incidence angles. The problem of spherical aberration can, in principle, easily be avoided by using the type of elliptical mirror that has been developed for x-ray focusing [22, 23]. With an elliptical mirror a spot width of  $0.45 \mu\text{m}$  is expected for  $w_{\text{S1}} = 5 \mu\text{m}$  and  $\lambda_{\text{dB}} = 0.56 \text{ \AA}$  at  $b_{\text{D}} = 10 \text{ cm}$ . When, in addition, a  $1 \mu\text{m}$  diameter micro-skimmer [7] is used to further reduce the effective source size, and when slit S2 is removed from the beam path, i.e. the effective diffracting width is given by the projection of the mirror along the incident beam direction ( $100 \mu\text{m}$  for  $\theta_{\text{in}} = 2 \text{ mrad}$ ), then a focal spot width of only  $90 \text{ nm}$  is expected.

#### 4. Conclusions and outlook

In summary, a helium atom beam has been focused to a spot width below  $2 \mu\text{m}$ , with very little background signal. The focal spot width decreases when the effective size of the helium beam source is reduced, when the image plane is moved closer to the mirror, and when the de Broglie wavelength of the atoms is shortened. By using two cylindrical mirrors of elliptical curvature in a KB arrangement it will be possible to achieve 2D focusing of a helium atom beam down to a

spot size of less than 100 nm (FWHM). We estimate the helium signal in such an arrangement to be on the order of 10 counts  $s^{-1}$ . This will allow for the realization of a helium atom microscope with superior resolution than that of a state-of-the-art classical light microscope. In this kind of microscope an object of interest is scanned through the atom beam focus and helium atoms, either transmitted or scattered sideways, are detected [4, 5]. Because of their low kinetic energy, thermal helium atoms are an exceptionally gentle probe and, unlike e.g. electrons or photons, cannot penetrate through the surface. Thus, as outlined by MacLaren *et al* [4], a scanning helium microscope would be non-destructive and perfectly surface-sensitive.

## Acknowledgments

BSZ acknowledges support from the Alexander von Humboldt Foundation and from the Korea Research Foundation Grant funded by the Korean Government (KRF-2005-214-C00188).

## References

- [1] Carnal O, Sigel M, Sleator T, Takuma H and Mlynek J 1991 Imaging and focusing of atoms by a Fresnel zone plate *Phys. Rev. Lett.* **67** 3231–4
- [2] Holst B and Allison W 1997 An atom-focusing mirror *Nature* **390** 244
- [3] Doak R B, Grisenti R E, Rehbein S, Schmahl G, Toennies J P and Wöll Ch 1999 Towards realization of an atomic de Broglie microscope: helium atom focusing using Fresnel zone plates *Phys. Rev. Lett.* **83** 4229–32
- [4] MacLaren D A, Holst B, Riley D J and Allison W 2003 Focusing elements and design considerations for a scanning helium microscope (SHeM) *Surf. Rev. Lett.* **10** 249–55
- [5] Kouznetsov D, Oberst H, Neumann A, Kuznetsova Y, Shimizu K, Bisson J F, Ueda K and Brueck S R J 2006 Ridged atomic mirrors and atomic nanoscope *J. Phys. B: At. Mol. Opt. Phys.* **39** 1605–23
- [6] Koch M, Rehbein S, Schmahl G, Reisinger T, Bracco G, Ernst W E and Holst B 2008 Imaging with neutral atoms—a new matter-wave microscope *J. Microsc.* **229** 1–5
- [7] Braun J, Day P K, Toennies J P, Witte G and Neher E 1997 Micrometer-sized nozzles and skimmers for the production of supersonic He atom beams *Rev. Sci. Instrum.* **68** 3001–9
- [8] Berkhout J J, Wolters E J, van Rooijen R and Walraven J T M 1986 Vanishing sticking probabilities and enhanced capillary flow of spin-polarized hydrogen *Phys. Rev. Lett.* **57** 2387–90
- [9] Yu I A, Doyle J M, Sandberg J C, Cesar C L, Kleppner D and Greytak T J 1993 Evidence for universal quantum reflection of hydrogen from liquid  $^4\text{He}$  *Phys. Rev. Lett.* **71** 1589–92
- [10] Berkhout J J, Luiten O J, Setija I D, Hijmans T W, Mizusaki T and Walraven J T M 1989 Quantum reflection: Focusing of hydrogen atoms with a concave mirror *Phys. Rev. Lett.* **63** 1689–92
- [11] Aminoff C G, Steane A M, Bouyer P, Desbiolles P, Dalibard J and Cohen-Tannoudji C 1993 Cesium atoms bouncing in a stable gravitational cavity *Phys. Rev. Lett.* **71** 3083–6
- [12] Hughes I G, Barton P A, Roach T M, Boshier M G and Hinds E A 1997 Atom optics with magnetic surfaces: I. Storage of cold atoms in a curved ‘floppy disk’ *J. Phys. B: At. Mol. Opt. Phys.* **30** 647–58
- [13] Oberst H, Morinaga M, Shimizu F and Shimizu K 2003 One-dimensional focusing of an atomic beam by a flat reflector *Appl. Phys. B* **76** 801–3
- [14] Hulpke E, Benedek G, Celli V and Comsa G (ed) 1992 *Helium Atom Scattering from Surfaces* (Berlin: Springer)
- [15] Oberst H, Kouznetsov D, Shimizu K, Fujita J and Shimizu F 2005 Fresnel diffraction mirror for an atomic wave *Phys. Rev. Lett.* **94** 013203
- [16] Shimizu F 2001 Specular reflection of very slow metastable neon atoms from a solid surface *Phys. Rev. Lett.* **86** 987–90

- [17] Friedrich H, Jacoby G and Meister C G 2002 Quantum reflection by Casimir-van der Waals potential tails *Phys. Rev. A* **65** 032902
- [18] Druzhinina V and DeKieviet M 2003 Experimental observation of quantum reflection far from threshold *Phys. Rev. Lett.* **91** 193202
- [19] Zhao B S, Schulz S A, Meek S A, Meijer G and Schöllkopf W 2008 Quantum reflection of helium atom beams from a microstructured grating *Phys. Rev. A* **78** 010902
- [20] Zhao B S, Schewe H C, Meijer G and Schöllkopf W 2009 Coherent reflection of He atom beams from rough surfaces at near-grazing incidence in preparation
- [21] Kirkpatrick P and Baez A V 1948 Formation of optical images by x-rays *J. Opt. Soc. Am.* **38** 766–74
- [22] Liu W, Ice G E, Tischler J Z, Khounsary A, Liu C, Assoufid L and Macrander A T 2005 Short focal length Kirkpatrick-Baez mirrors for a hard x-ray nanoprobe *Rev. Sci. Instrum.* **76** 113701
- [23] Yumoto H *et al* 2005 Fabrication of elliptically figured mirror for focusing hard x rays to size less than 50 nm *Rev. Sci. Instrum.* **76** 063708
- [24] Bruch L W, Schöllkopf W and Toennies J P 2002 The formation of dimers and trimers in free jet  $^4\text{He}$  cryogenic expansions *J. Chem. Phys.* **117** 1544–66
- [25] Grisenti R E, Schöllkopf W, Toennies J P, Manson J R, Savas T A and Smith H I 2000 He-atom diffraction from nanostructure transmission gratings: the role of imperfections *Phys. Rev. A* **61** 033608